Nazarii Danyliuk, Tetiana Tatarchuk, Ivan Mironyuk, Volodymyr Kotsyubynsky, Volodymyr Mandzyuk

Performance of commercial titanium dioxide samples in terms of dye photodegradation assessed using smartphone-based measurements

Vasyl Stefanyk Precarpathian National University, Ivano-Frankivsk, Ukraine, danyliuk.nazariy@gmail.com

The photocatalytic activity of four titanium dioxide samples (TiO_2-P25 Degussa, PC105 Millennium, PC500 Millennium, and Anatase) was studied in the degradation of dyes (Congo Red (CR), Methyl Orange (MO), and Direct Red 23 (DR23)) using cost-effective smartphone-based analysis. The obtained kinetic curves are well described by the first-order kinetic model. It was established that the phase composition, the size of the particles, and the specific surface area of the catalyst have a significant effect on the photocatalytic activity of the studied TiO_2 samples. It was investigated that the Millennium PC500 sample is the most effective photocatalyst due to a large specific surface area and a small particle size (8 nm). TiO_2-P25 Degussa and Anatase also demonstrate a high photocatalytic activity in the degradation of CR and DR23 dyes, which can be explained by the accelerated process of electron transfer between the anatase and rutile phases. For the PC105 sample, a higher CR photodegradation efficiency is observed compared to PC500. It can be concluded that heterogeneous photocatalysis is an effective method for the removal of toxic dyes from wastewater. With the use of smartphone-based analysis, it is possible monitoring the photodegradation kinetics in real-time.

Keywords: dye; photocatalysis; smartphone-based analysis; titania.

Received 17 June 2022; Accepted 12 September 2022.

Introduction

The fast progress of the textile and paper industry has led to the disposal problem with a large number of organic pollutants, which are harmful to the environment and human health. About 15% of the dyes (mostly azo dyes) are lost during use, end up in the wastewaters, and create serious problems releasing carcinogenic substances into the aquatic environment [1]. Therefore, it is very important to develop effective methods of wastewater treatment from harmful substances.

Recently, different advanced oxidation processes (AOPs) have been developed to overcome the growing problem [2]. The key mechanism of AOPs consists of the formation of active hydroxyl radicals, which can destroy the organic pollutants in wastewater. One of the types of AOPs is heterogeneous photocatalysis, which allows the destruction of toxic substances under UV light, up to the formation of CO_2 and H_2O molecules [3,4]. The heterogeneous process involves a solid semiconductor (in powder form), oxygen as an electron acceptor, and light as an energy source. Because of light illumination, the electrons from the valence band of the semiconductor are excited and move to the conduction band, while positively charged holes remain in it. The formed electron-hole pairs lead to the occurrence of redox reactions on the photocatalyst surface [5]. Accordingly, the higher the energy of the formed electron-hole pairs, the more efficient the semiconductor.

Nowadays, TiO_2 is the most effective photocatalyst for the photodegradation of organic dyes due to the high redox potential of photogenerated holes on its surface [6]. The main advantages of TiO_2 are environmental friendliness, photo corrosion resistance, chemical stability, availability, and low cost [7]. TiO_2 exists in

various crystalline forms; the most common forms are anatase and rutile. The band gap of anatase is 3.2 eV, while the band gap of rutile is 3.0 eV. Therefore, the anatase is a better photocatalyst compared to rutile [8]. However, it was found that a mixture of polymorphs exhibits a synergistic effect and increased photocatalytic activity compared to pure phases [9,10]. The reason is that the accelerated charge transfer process causes a positive effect.

It is known that the photocatalytic activity of TiO_2 depends on a set of factors such as phase structure, crystallite size, specific surface area, and pore structure [11,12]. Many different types of commercial catalysts are commonly used in photocatalytic reactions, including TiO_2 Degussa P25 (Evonik) and Millennium PCs catalysts (Millennium Chemicals). The catalyst Degussa P25 consists of both anatase and rutile phases. The catalysts labeled as Millennium PCs are consists of anatase phase and differ in specific surface area, particle size, etc. However, to date, there are not so many studies on the efficiency of Millennium PCs catalysts in photocatalytic reactions.

For example, in work [13] photodegradation of Methyl Orange (MO) dye was investigated using Degussa P25 and Millennium PC500 TiO_2 samples under UV light. The effect of pH and H_2O_2 (as electron acceptors) on the efficiency of photocatalysts was investigated. It was determined that photooxidation was significantly enhanced in the presence of hydrogen peroxide. The pH of the solution had a direct effect on MO adsorption on the surface of the photocatalyst, in particular, a significant increase was observed in an acidic medium.

The optimization of Reactive Green 19 (RG19) photodegradation was carried out in work [14] under UV light using Millennium PC-500 TiO_2 nanoparticles (with crystallite size of 8 nm), immobilized on ceramic plates for a flow photoreactor. The maximum decolorization efficiency of RG19 was achieved under the following conditions: the initial concentration of the dye of 10 mg/L, a feed rate of 150 mL/min, the intensity of UV light of 47.2 W/m^2, and the reaction time of 240 min.

The photocatalytic degradation of a mixture of three pharmaceuticals: Metronidazole (MET), Atenolol (ATL), and Chlorpromazine (CPR) is described in work [15]. The Millennium PC-500 photocatalyst was immobilized by the sol-gel method on ceramic plates. The work determined the optimal initial concentration of three pharmaceuticals, the reaction time, and the intensity of UV light, which are equal to 10 mg/L, 150 min, and 38.45 W/m^2, respectively. Chronic toxicity of remaining pharmaceuticals was evaluated using *Spirodela polyrrhiza* before and after the photocatalytic experiments. The results of TOC (90% removal within 16 h) and toxicology experiments showed that photocatalysis can effectively mineralize and reduce the toxicity of pharmaceuticals in aqueous solutions.

This work aims to investigate the photocatalytic degradation of Congo Red (CR), Methyl Orange (MO), and Direct Red 23 (DR23) dyes using commercial titanium dioxide samples (Degussa P25, Millennium PC105, Millennium PC500, and Anatase) and the smartphone-based analysis for real-time monitoring of photodegradation kinetics.

I. Experimental

1.1. Materials and characterization

The TiO_2 photocatalysts were commercial Aeroxide TiO_2 P25, Millennium PC105, Millennium PC500, and Anatase. Aeroxide TiO_2 P25 was received from Evonik (Germany). Millennium PC105 and Millennium PC500 samples were obtained from Millenium Inorganics (Belgium). Anatase (CAS 1317-70-0, nanopowder, < 25 nm particle size, 99.7% trace metals basis) was obtained from Sigma-Aldrich (Germany). Congo Red and Methyl Orange dyes were of analytical grade. Direct Red 23 dye (CAS 3441-14-3, technical grade) was obtained from Boruta (Poland).

XRD patterns were obtained using the Shimadzu XRD-7000 diffractometer operating in the Bragg-Brentano mode with Cu-Kα radiation (30 kV, 30 mA) and diffracted beam monochromator, using a step scan mode with the step of 0.02° (2θ). The instrumental resolution function (IRF) of the diffractometer was calculated by the fitting of the XRD pattern of a LaB_6 NIST standard, which was measured under the same experimental conditions as the investigated samples. All diffraction patterns were compared concerning crystallography open database (COD) and PDF2 databases. The molar fraction of rutile was determined using Rietveld refinement of experimental XRD patterns with FullProff/Match! software. The average crystallite sizes were calculated using the Scherrer equation with the Warren constant taken as 0.90.

1.2. Photodegradation experiments

The micro-photoreactor has been described in detail in our previous articles [11,16]. The UV LED (3 W) was a source of UV light. Congo Red (CR), Methyl Orange (MO), and Direct Red 23 (DR23) dyes were used as model dyes due to their insignificant absorption in the UV range. Therefore, UV light with a wavelength of 365 nm does not cause photolytic degradation of dyes. The cuvette with a precise volume (20 mL) was filled with a solution of CR, MO, and DR23 dyes (5 mg/L). Then a photocatalyst powder (30 mg) was added to the cuvette. The pH of dyes solutions was equal to 6.3. The reaction mixture was stirred in the dark for 15 min to achieve adsorption-desorption equilibrium on the TiO_2 surface. Then UV light was turned on for 30 min. Blank experiments (without UV light) showed the absence of dye adsorption on the TiO_2 surface. The photocatalyst surface remains white after centrifugation at 4000 rpm for 10 min, which evidences that there are no undecomposed CR, MO, and DR23 dyes on the TiO_2 surface.

Kinetic curves of CR, MO, and DR23 dyes photodegradation were recorded using an iPhone 8 Plus smartphone (MQ8Y2LL/A model). After the specified time intervals, the microreactor was opened and the image of the reaction mixture was recorded. The measurement process is described in detail in previous work [16]. As a result of the degradation of CR, MO, and DR23 dyes, the reaction mixture changes its color from bright red to white. The RGB values of the registered images were obtained using the Color Name AR software. The residual concentrations of Congo Red (CR), Methyl Orange (MO), and Direct Red 23 (DR23) dyes in the solutions were

Nazarii Danyliuk, Tetiana Tatarchuk, Ivan Mironyuk, Volodymyr Kotsyubynsky, Volodymyr Mandzyuk

determined at 505, 470, and 510 nm for CR, MO, and DR23, respectively using a UV-vis spectrophotometer ULAB 102-UV (Fig. 1a-c). The obtained calibration curves are presented in Fig. 1d-f, which are characterized by high correlation coefficients (R^2=0.9975-0.9997) in wide concentration ranges from 1 to 50 mg/L, from 2.5 to 50 mg/L, and from 1 to 100 mg/L for CR, MO, and DR23 respectively. The degree of dye degradation was calculated according to the formula:

[degradation degree, %] = $100 \times (C_0 - C_f) / C_0$,

where C_0 and C_f are initial and final dye concentrations.

II. Results and discussion

2.1. XRD analysis

The differences in phase composition and morphologies of commercial TiO_2 photocatalysts are observed in their XRD patterns (Fig. 2). XRD pattern of the P25 sample exhibited diffraction peaks of anatase (COD #96-900-8214) and rutile (COD #96-900-4143) without amorphous TiO_2 observed in the literature [17]. According to Rietveld refinement, the phase composition of TiO_2 P25 is 86.3 % (mol.) of anatase and 13.7 % (mol.) of rutile. The calculated cell parameters of tetragonal TiO_2 anatase phase (space group I41/amd) are $a = b = 3.7817$ Å and $c = 9.4986$ Å. The average size of crystallites for the anatase phase component (estimated from the corrected FWHM of the reflections using the Scherrer equation) is in the range of about 20-22 nm.

The XRD spectra of the Anatase sample also indicate the rutile component presence (up to 5 mol. %). Cell parameters of the anatase phase are $a = b = 3.7842$ Å and $c = 9.5026$ Å, the average crystallite size for the anatase phase is about 25 nm.

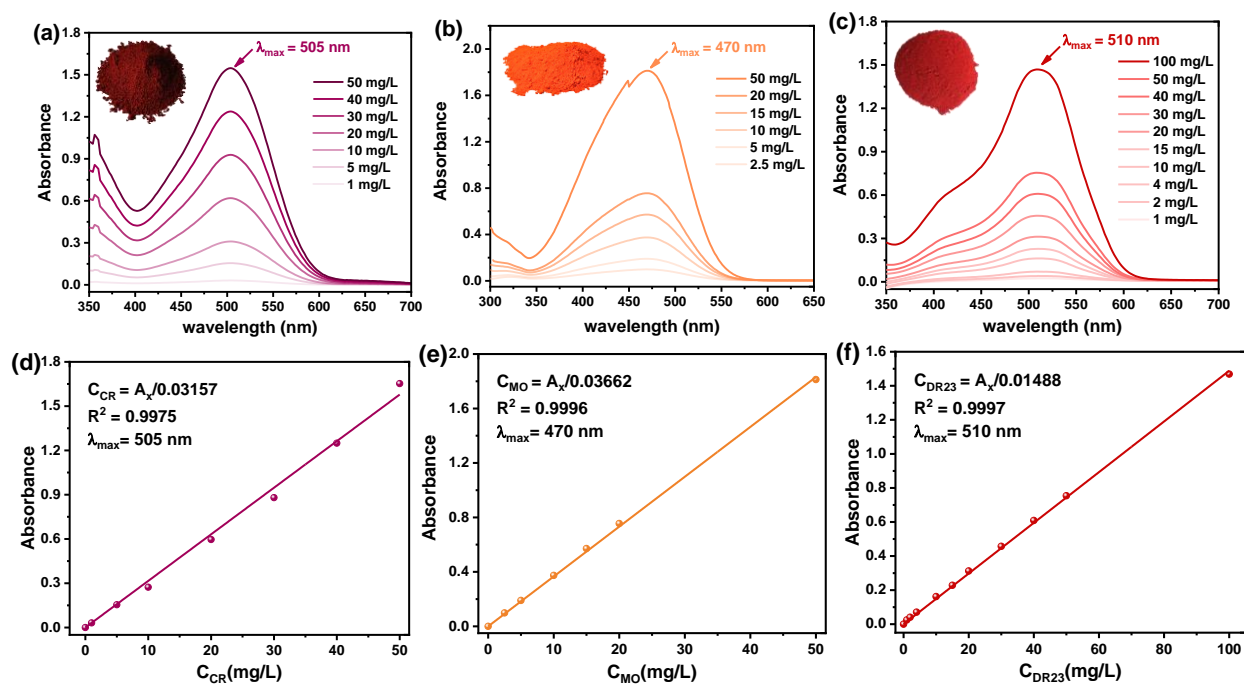Both Millennium PC catalysts were single-phase

Fig. 1. UV-vis spectra of (a) CR, (b) MO, and (c) DR23 solutions at indicated concentrations. Absorbance at 505, 470, and 510 nm (the spectral peak wavelength) versus (d) CR, (e) MO, and (f) DR23 concentration.

Table 1

Characteristics of the dyes used for the photocatalytic experiments.

Dye	M, g/mol	λ_{max}, nm	Chemical structure
Congo Red (CR)	696.66	505	
Methyl Orange (MO)	327.33	470	
Direct Red 23 (DR23)	813.71	510	

anatase with an average particle size of 22-24 nm and about 8 nm for PC105 and PC500 samples, respectively. Cell parameters for PC105 (a = 3.7832 and c = 9.5058 Å) and PC500 (a = 3.7904 Å and c = 9.5024 Å) samples are close.
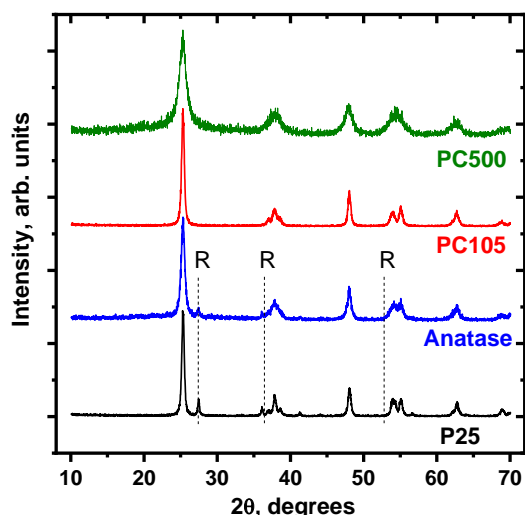

Fig. 2. XRD patterns of commercial TiO$_2$ samples: Degussa P25, Millennium PC105, Millennium PC500, and Anatase.

Table 2

The phases, crystallite size, and surface area of the photocatalysts.

Photocatalyst	Composition (%) anatase / rutile	Surface area (m^{2}g^{-1})	Crystallite size (nm)
P25	86.3 / 13.7	50	20
PC105	100 / 0	80	24
PC500	100 / 0	345	8
Anatase	95 / 5		<25

2.2. Photodegradation studies

Smartphone-based analysis was used for obtaining calibration curves for Congo Red (CR), Methyl Orange (MO), and Direct Red 23 (DR23) dyes. Calibration points were measured by stepwise addition of a concentrated dye solution directly into the reaction mixture with the following color images captured by a smartphone. The obtained color images and corresponding RGB values were processed as described in works [11,16]. The red color (R) among the RGB data turned out to be the most suitable for determining the CR, MO, and DR23 dyes

concentration (Fig. 3). The obtained calibration curves (Fig. 3a-c) are well described by second-order polynomial equations (Table 3). The calibration coefficients depend on both the type of photocatalyst and the dye concentration. The high values of the correlation coefficients R^2 (0.9610-0.9965) confirm the reliability of dye concentration estimating using a smartphone.

Kinetic curves of CR, MO, and DR23 dyes photodegradation are presented in Fig. 4a-c. Semi-logarithmic lines are presented in Fig. 4d-f. A first-order kinetic equation can be used to describe the obtained experimental data. The calculated values of the reaction rate constants are presented in Table 4. The corresponding values of the correlation coefficient (R^2) are in the range of 0.9278 to 0.9947 (Table 4). High R^2 values confirm the correct application of the first-order kinetic model. To confirm and compare the obtained data, the residual concentration of CR, MO, and DR23 dyes was determined using absorbance at 505, 470, and 510 nm, respectively. The obtained spectra are presented in Fig. 5a-c. The values of the degree of photodegradation efficiency are presented in Fig. 5d-f. In general, the dose of 1.5 g/L of photocatalysts provides almost complete photodegradation of CR, MO, and DR23 dyes under UV light for 30 minutes (Fig. 5d-f).

The most effective samples for CR, MO, and DR23 dyes photodegradation were determined using the analysis of rate constants. For the photodegradation of CR, the most effective photocatalyst is the PC105 sample (a reaction rate constant of 0.0915 min^{-1}). During MO photodegradation, the highest reaction rate constant of 0.1810 min^{-1} has been obtained for the PC500 sample. PC500 and P25 samples showed the same photodegradation efficiency of DR23: reaction rate constants of 0.0688 min^{-1} and 0.0622 min^{-1}, respectively.

It is known that the photocatalytic activity of the TiO$_2$ samples depends on the main structural properties, such as the crystal composition (anatase or rutile phases), specific surface area, band gap, porosity, and particle size distribution [13,18,19]. The studied photocatalysts can be placed in the following order by their efficiency: PC105 > Anatase > PC500 > P25 for CR photodegradation; PC500 > P25 > PC105 > Anatase for MO photodegradation; PC500 > Anatase > PC105 > P25 for DR23 photodegradation. These results indicate that the surface and structural properties of photocatalysts play a major role in dye photodegradation. It was experimentally determined that photodegradation of MO and DR23 dyes occurred much faster in the presence of Millennium PC500 compared to other photocatalysts. A large specific
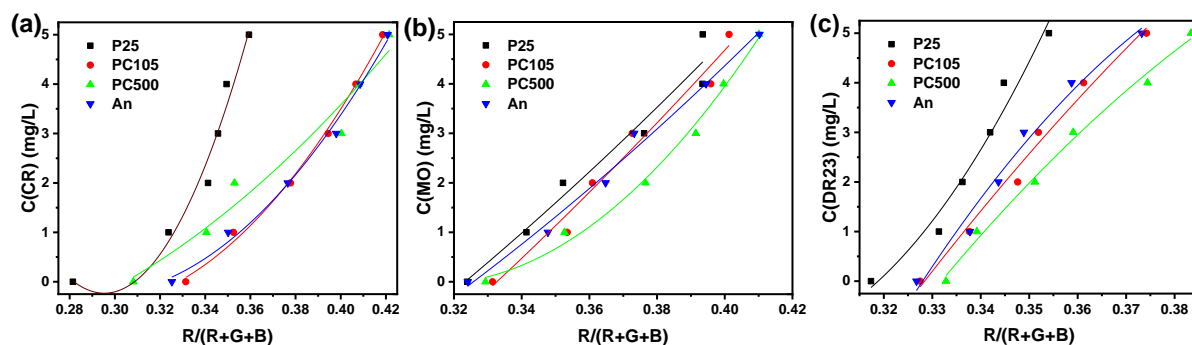

Fig. 3. The calibration lines for (a) CR, (b) MO, and (c) DR23.

Table 3

The calibration equations for the CR, MO, and DR23 dyes.

| Photocatalyst	Calibration equation	R^2
Congo Red		
P25	$C_{CR} = 1290.89 * Red^2 - 762.40 * Red + 112.33$	0.9721
PC105	$C_{CR} = 324.95 * Red^2 - 188.00 * Red + 26.70$	0.9965
PC500	$C_{CR} = 117.99 * Red^2 - 45.58 * Red + 2.93$	0.9610
Anatase	$C_{CR} = 306.00 * Red^2 - 178.01 * Red + 25.62$	0.9933
Methyl Orange		
P25	$C_{MO} = 83.93 * Red^2 + 3.12 * Red - 9.78$	0.9625
PC105	$C_{MO} = 82.92 * Red^2 + 8.75 * Red - 12.08$	0.9747
PC500	$C_{MO} = 532.80 * Red^2 - 333.97 * Red + 52.28$	0.9933
Anatase	$C_{MO} = 94.23 * Red^2 - 9.60 * Red - 6.86$	0.9897
Direct Red 23		
P25	$C_{DR23} = 1672.85 * Red^2 - 976.95 * Red + 141.43$	0.9697
PC105	$C_{DR23} = -308.63 * Red^2 + 328.35 * Red - 74.54$	0.9872
PC500	$C_{DR23} = -426.32 * Red^2 + 399.83 * Red - 85.74$	0.9931
Anatase	$C_{DR23} = -791.87 * Red^2 + 668.11 * Red - 133.94$	0.9831
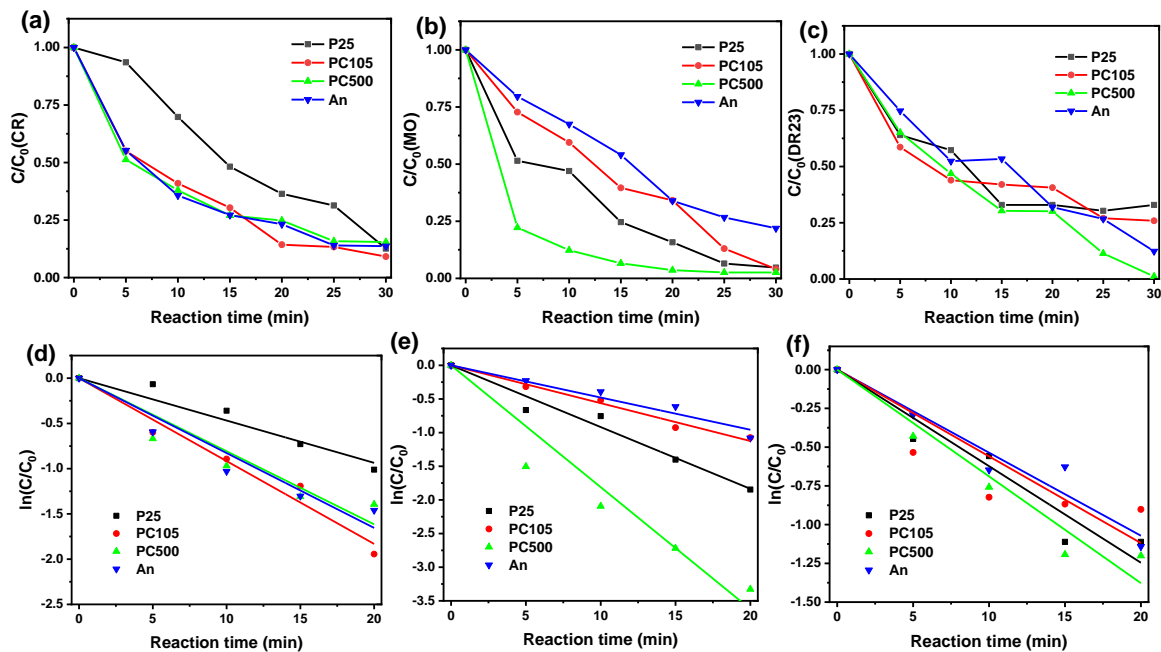
Fig. 4. Kinetic lines of photodegradation (a) CR, (b) MO, (c) DR23; semi-logarithmic transformations of the kinetic lines: (d) CR, (e) MO, and (f) DR23.

Table 4

Rate constants of the first-order kinetic model.

Photocatalyst	Congo Red		Methyl Orange		Direct Red 23	
	k (min^{-1})	R^2	k (min^{-1})	R^2	k (min^{-1})	R^2
P25	0.0467	0.9726	0.0917	0.9891	0.0622	0.9758
PC105	0.0915	0.9896	0.0562	0.9947	0.0559	0.9278
PC500	0.0807	0.9694	0.1810	0.9790	0.0688	0.9810
An	0.0827	0.9781	0.0478	0.9809	0.0535	0.9778

surface area (345 m^2/g) and a smaller particle size (8 nm) can explain the better photocatalytic activity. Millennium PC105 proved to be the most effective catalyst for CR photodegradation, despite its lower specific surface area (80 m^2/g). However, PC105 exhibits a slow rate for MO and DR23 photodegradation. Thus, it is shown that a large surface area of PC500 does not give a higher photocatalytic activity; other factors also play an important role. Anatase photocatalyst, which consists from 95% of anatase and 5% of rutile, was found to be the second most effective catalyst after PC500 for the CR and DR23 photodegradation. The Degussa P25 catalyst demonstrates better activity for the MO photocatalytic degradation and a large number of organic compounds
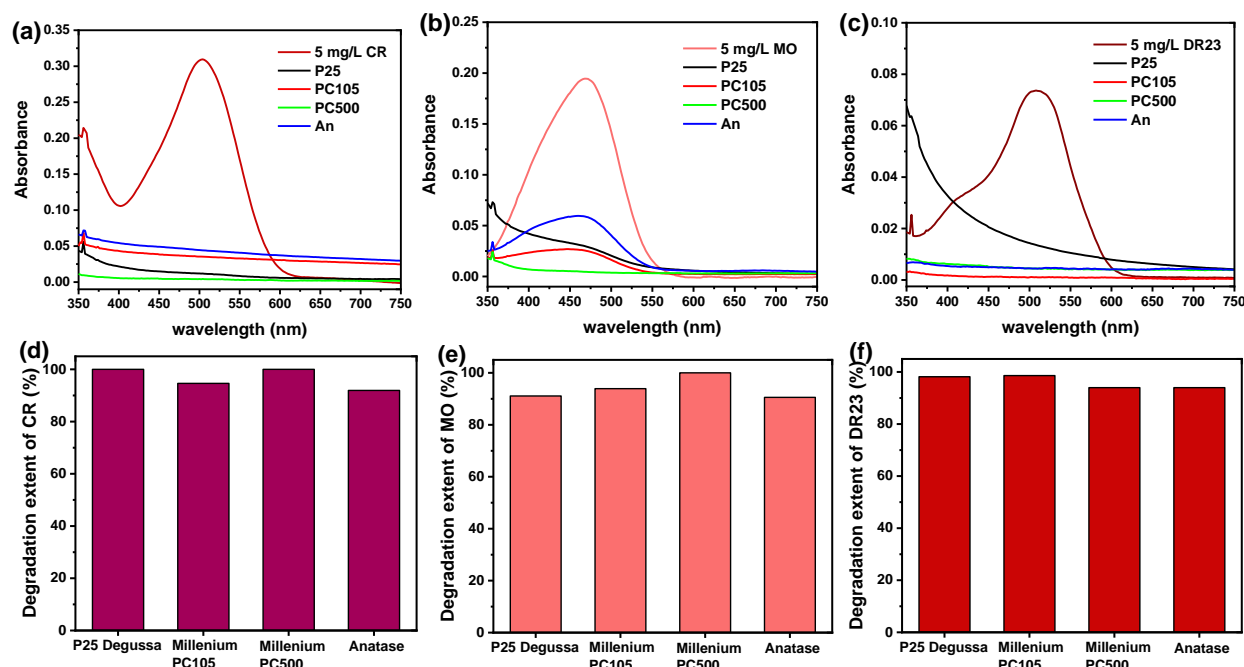
Fig. 5. UV–Vis spectra of (a) CR, (b) MO, and (c) DR23 dye solutions; Degradation efficiency of (d) CR, (e) MO, and (f) DR23 dyes.

[11,20]. The high photocatalytic activity of Anatase and P25 photocatalysts can be explained by the fact that they are mixed-phase samples. In particular, sample P25 consists of small rutile nanocrystallites dispersed inside the anatase matrix [21]. The band gaps of anatase and rutile TiO_2 are 3.20 eV and 3.03 eV, respectively [22]. The lower energy of the band gap for the rutile allows it to interact with light photons, forming an electron-hole pair. As a result, there is a rapid transfer of electrons from the conduction band of the rutile to the electron traps of anatase. Thus, the recombination of the formed pairs is inhibited, allowing the hole to move to the surface of the catalyst particles and take part in the process.

Conclusions

The results showed that photocatalysis is an effective method for dye removal from wastewater. The determination of the photocatalytic activity of TiO_2 Degussa P25, PCs Millennium (PC105 and PC500), and Anatase samples was carried out during the photodegradation of Congo Red (CR), Methyl orange (MO), and Direct Red 23 (DR23) dyes. Kinetic curves were recorded using an iPhone 8 Plus smartphone. The photodegradation processes are well described by the first-order kinetic model. It was determined that the efficiency of the process strongly depends on the experimental conditions and the type of photocatalyst. The Millennium PC500 sample with smaller particles and higher surface area showed the best photodegradation performance of MO and DR23 dyes compared to the other samples. The PC105 sample turned out to be the most effective catalyst for the photodegradation of CR, despite its small specific surface area. Two-phase TiO_2 photocatalysts (Degussa P25 and Anatase) were found to have higher CR and DR23 degradation activity than single-phase TiO_2 (PC Millennium), which can be explained by the electronic interaction between anatase and rutile phases. The presented TiO_2 photocatalysts are very effective materials for the degradation of azo dyes under UV light action. The smartphone-based analysis can be used for monitoring the photodegradation kinetics in real time.

Nazarii Danyliuk – PhD student, leading specialist at the Educational and Scientific Center of Material Science and Nanotechnology, Vasyl Stefanyk Precarpathian National University;

Tetiana Tatarchuk – Associate Professor of the Chemistry Department, Director of Educational and Scientific Center of Materials Science and Nanotechnology, Vasyl Stefanyk Precarpathian National University;

Ivan Mironyuk – Doctor of Chemical Sciences, Head of the Department of Chemistry, Vasyl Stefanyk Precarpathian National University;

Volodymyr Kotsyubynsky – Doctor of Physical and Mathematical Sciences, Vasyl Stefanyk Precarpathian National University;

Volodymyr Mandzyuk – Doctor of Physical and Mathematical Sciences, Associate Professor of the Department of Computer Engineering and Electronics, Vasyl Stefanyk Precarpathian National University.

[1] Y.H. Chiu, T.F.M. Chang, C.Y. Chen, M. Sone, Y.J. Hsu, Mechanistic insights into photodegradation of organic dyes using heterostructure photocatalysts, Catalysts 9, 430 (2019); https://doi.org/10.3390/catal9050430.

[2] Y. Deng, R. Zhao, Advanced Oxidation Processes (AOPs) in Wastewater Treatment, Curr. Pollut. Reports 1, 167 (2015); https://doi.org/10.1007/s40726-015-0015-z.

[3] K. Rajeshwar, M.E. Osugi, W. Chanmanee, C.R. Chenthamarakshan, M.V.B. Zanoni, P. Kajitvichyanukul, R. Krishnan-Ayer, Heterogeneous photocatalytic treatment of organic dyes in air and aqueous media, J. Photochem. Photobiol. C Photochem. Rev 9, 171 (2008); https://doi.org/10.1016/j.jphotochemrev.2008.09.001.

[4] C.M. Mistura, I.A.H. Schneider, Y. Vieira, Heterogeneous Photocatalytic Degradation of Dyes in Water/Alcohol Solution Used by the Brazilian Agate Industry, Geomaterials 09, 29 (2019); https://doi.org/10.4236/gm.2019.91003.

[5] M. Bodzek, M. Rajca, Photocatalysis in the treatment and disinfection of water, Ecol. Chem. Eng. S 19, 489 (2012); https://doi.org/10.2478/v10216-011-0036-5.

[6] N.K. Jangid, S. Jadoun, A. Yadav, M. Srivastava, N. Kaur, Polyaniline-TiO_2-based photocatalysts for dyes degradation, 2021; https://doi.org/10.1007/s00289-020-03318-w.

[7] S. Al Jitan, G. Palmisano, C. Garlisi, Synthesis and surface modification of TiO_2-based photocatalysts for the conversion of CO_2, Catalysts 10, (2020); https://doi.org/10.3390/catal10020227.

[8] J. Zhang, P. Zhou, J. Liu, J. Yu, New understanding of the difference of photocatalytic activity among anatase, rutile and brookite TiO_2, Phys. Chem. Chem. Phys 16, 20382 (2014); https://doi.org/10.1039/c4cp02201g.

[9] Z. Rui, S. Wu, C. Peng, H. Ji, Comparison of TiO_2 Degussa P25 with anatase and rutile crystalline phases for methane combustion, Chem. Eng. J. 243, 254 (2014); https://doi.org/10.1016/j.cej.2014.01.010.

[10] N. Bouanimba, N. Laid, R. Zouaghi, T. Sehili, A Comparative Study of the Activity of TiO_2 Degussa P25 and Millennium PCs in the Photocatalytic Degradation of Bromothymol Blue, Int. J. Chem. React. Eng 16, 1 (2018); https://doi.org/10.1515/ijcre-2017-0014.

[11] N. Danyliuk, T. Tatarchuk, K. Kannan, A. Shyichuk, Optimization of TiO_2-P25 photocatalyst dose and H_2O_2 concentration for advanced photooxidation using smartphone-based colorimetry, Water Sci. Technol 84, 469 (2021); https://doi.org/10.2166/wst.2021.236.

[12] T. Tatarchuk, N. Danyliuk, A. Shyichuk, W. Macyk, M. Naushad, Photocatalytic degradation of dyes using rutile TiO_2 synthesized by reverse micelle and low temperature methods: real-time monitoring of the degradation kinetics, J. Mol. Liq 342, 117407 (2021); https://doi.org/10.1016/j.molliq.2021.117407.

[13] N. Bouanimba, N. Laid, R. Zouaghi, T. Sehili, Effect of pH and inorganic salts on the photocatalytic decolorization of methyl orange in the presence of TiO_2 P25 and PC500, Desalin. Water Treat 53, 951 (2015); https://doi.org/10.1080/19443994.2013.848667.

[14] P. Taylor, M. Rastegar, K.R. Shadbad, A.R. Khataee, R. Pourrajab, Optimization of photocatalytic degradation of sulphonated diazo dye C. I. Reactive Green 19 using ceramic-coated TiO_2 nanoparticles, (n.d.) 37–41; https://doi.org/10.1080/09593330.2011.604859.

[15] A.R. Khataee, M. Fathinia, S.W. Joo, Simultaneous monitoring of photocatalysis of three pharmaceuticals by immobilized TiO_2 nanoparticles: Chemometric assessment , intermediates identification and ecotoxicological evaluation, Spectrochim. Acta Part A Mol. Biomol. Spectrosc 112, 33 (2013); https://doi.org/10.1016/j.saa.2013.04.028.

[16] N. Danyliuk, T. Tatarchuk, A. Shyichuk, Estimation of Photocatalytic Degradation Rate Using Smartphone Based Analysis, Phys. Chem. Solid State 4, 727 (2020); https://doi.org/10.15330/pcss.21.4.727-736.

[17] P. Apopei, C. Catrinescu, C. Teodosiu, S. Royer, Mixed-phase TiO_2 photocatalysts: Crystalline phase isolation and reconstruction, characterization and photocatalytic activity in the oxidation of 4-chlorophenol from aqueous effluents, Appl. Catal. B Environ, 160–161, 374 (2014); https://doi.org/10.1016/j.apcatb.2014.05.030.

[18] A.R. Khataee, H. Aleboyeh, A. Aleboyeh, Crystallite phase-controlled preparation, characterisation and photocatalytic properties of titanium dioxide nanoparticles, J. Exp. Nanosci 4, 121 (2009); https://doi.org/10.1080/17458080902929945.

[19] S. Estrada-Flores, A. Martínez-Luévanos, C.M. Perez-Berumen, L.A. García-Cerda, T.E. Flores-Guia, Relationship between morphology, porosity, and the photocatalytic activity of TiO_2 obtained by sol–gel method assisted with ionic and nonionic surfactants, Bol. La Soc. Esp. Ceram. y Vidr. 59, 209 (2020); https://doi.org/10.1016/j.bsecv.2019.10.003.

[20] W.Q. Yap, Y.H. Chin, K.H. Leong, P. Saravanan, L.C. Sim, Design of photoreactor with high sunlight concentration for improved photocatalytic degradation of dye pollutant, IOP Conf. Ser. Earth Environ. Sci. 646 (2021); https://doi.org/10.1088/1755-1315/646/1/012012.

[21] S. Topcu, G. Jodhani, P.I. Gouma, Optimized nanostructured TiO_2 photocatalysts, Front. Mater. 3, 1 (2016); https://doi.org/10.3389/fmats.2016.00035.

[22] D.O. Scanlon, C.W. Dunnill, J. Buckeridge, S.A. Shevlin, A.J. Logsdail, S.M. Woodley, C.R.A. Catlow, M.J. Powell, R.G. Palgrave, I.P. Parkin, G.W. Watson, T.W. Keal, P. Sherwood, A. Walsh, A.A. Sokol, Band alignment of rutile and anatase TiO_2, Nat. Mater. 12, 798 (2013); https://doi.org/10.1038/nmat3697.

Назарій Данилюк, Тетяна Татарчук, Іван Миронюк, Володимир Коцюбинський, Володимир Мандзюк

Ефективність комерційних зразків діоксиду титану у фотодеградації барвників, визначена за допомогою смартфону

Прикарпатський національний університет імені Василя Стефаника, Івано-Франківськ, Україна,
danyliuk.nazariy@gmail.com

Досліджено фотокаталітичну активність чотирьох зразків титан діоксиду (TiO$_2$-P25 Degussa, PC105 Millennium, PC500 Millennium та Anatase) під час деградації барвників (Конго Червоного (КЧ), Метилоранжу (МО) та Direct Red 23 (DR23)) з використанням смартфону. Отримані кінетичні криві добре описуються кінетичною моделлю першого порядку. Встановлено, що фазовий склад, розмір частинок і питома площа поверхні каталізатора мають значний вплив на фотокаталітичну активність досліджуваних зразків TiO$_2$. Досліджено, що зразок Millennium PC500 є найефективнішим фотокаталізатором завдяки великій питомій площі поверхні та малому розміру частинок (8 нм). Зразки TiO$_2$-P25 Degussa та Anatase також демонструють високу фотокаталітичну активність під час деградації барвників КЧ та DR23, що можна пояснити прискореним процесом перенесення електронів між фазами анатазу та рутилу. Для зразка PC105 спостерігається вища ефективність фотодеградації КЧ порівняно з PC500. Можна зробити висновок, що гетерогенний фотокаталіз є ефективним методом видалення токсичних барвників зі стічних вод. За допомогою аналізу на основі смартфону можна контролювати кінетику фотодеградації барвників в режимі реального часу.

Ключові слова: барвник; фотокаталіз; аналіз на основі смартфону; титан (IV) оксид.